

has been kindly supplied by Dr. A. Temkin.

¹³K. Bell and A. Kingston, Proc. Phys. Soc. (London) **90**, 31 (1967).

¹⁴P. Lee and G. L. Weissler, Astrophys. J. **115**, 570 (1952).

¹⁵E. N. Lassette and E. A. Jones, J. Chem. Phys. **40**, 1222 (1964).

¹⁶Curves C and Z of the present investigation are identical, respectively, to the curves 1 and 2 of the figure on page 626 of the abstracts for the Fifth International Conference on the Physics of Electronic and Atomic Collisions, Leningrad, 1967, edited by E. Levowitz (Nauka, Leningrad, 1968). However, due to a computational error, the values represented by curve 1 are incorrect.

Remeasurement of the Lamb Shift in D, $n = 2$ ^{*†}

B. L. Cosens

Yale University, New Haven, Connecticut

(Received 26 April 1968)

The Lamb shift in the $n = 2$ level of deuterium has been measured by locating the crossing point of the levels $2^2S_{1/2}$ ($m_J = -1/2$) and $2^2P_{1/2}$ ($m_J = +1/2$) near 574 G. An atomic beam in the metastable $2^2S_{1/2}$ state was prepared, having a single hyperfine structure component. This beam then traveled into a magnetic field where a static electric field was used to induce transitions to the $2^2P_{1/2}$ ($m_J = +1/2$) state. Transitions utilizing two different hyperfine components were measured, and yielded two independent values of the Lamb shift. Eleven corrections to the data are discussed in some detail. The final value for the Lamb shift is $\delta_D = 1059.24 \pm 0.10$ MHz. This result disagrees slightly with the original measurement of Lamb *et al.*, but does agree with the most recent theoretical result.

I. INTRODUCTION

The determination of the Lamb shift is one of the most important tests of quantum electrodynamics. Recent remeasurements¹⁻³ have given a value for the Lamb shift in the $n = 2$ level of hydrogen, and this paper reports a remeasurement of the Lamb shift in the $n = 2$ level of deuterium.

In a series of microwave atomic beam experiments, Lamb and his co-workers⁴ measured the fine structure (fs) of the $n = 2$ levels of hydrogen and deuterium. These experiments provided values for the fine structure constant α and the Lamb shift δ . The experiments to be described here are part of a series¹⁻³ designed to remeasure this fs in H and D. These experiments will eventually yield a redetermination of α .

In these experiments, we have located the crossing point of the metastable $2^2S_{1/2}$ level β with the short-lived $2^2P_{1/2}$ level e near 574 G (see Fig. 1). Measurement of the crossing-point magnetic field along with a detailed knowledge of the Zeeman energy levels determines the Lamb shift δ .

II. GENERAL PROCEDURE AND APPARATUS

The Zeeman energy of the $2^2S_{1/2}$ and $2^2P_{1/2}$ levels (including the hyperfine structure for deuterium in the inset) is shown in Fig. 2. The crossing-point technique is discussed in detail in Ref. 1. Briefly, it consists of the following: A beam of atoms in the $2S$ state α is produced from ground-state molecules by thermal dissociation followed by electron bombardment in a 574-G mag-

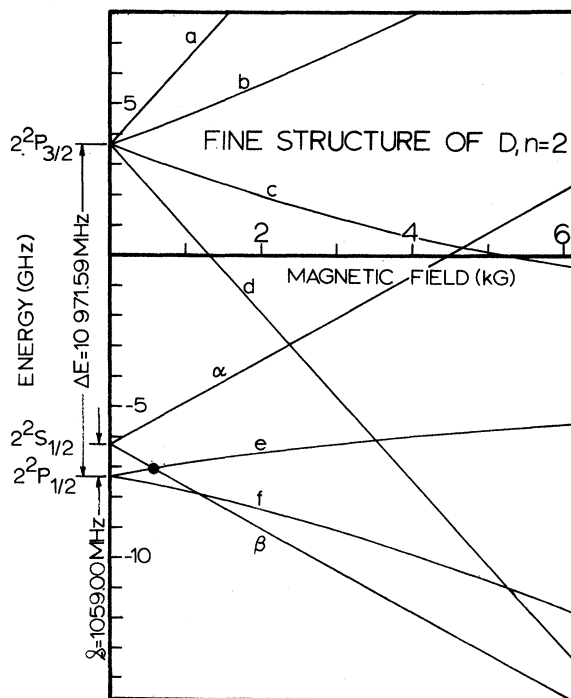


FIG. 1. Zeeman diagram of the fine structure of D, $n = 2$. The zero-field separations are the values obtained by Lamb *et al.* This experiment locates the crossing of the levels β and e near 574 G, indicated by the dot.

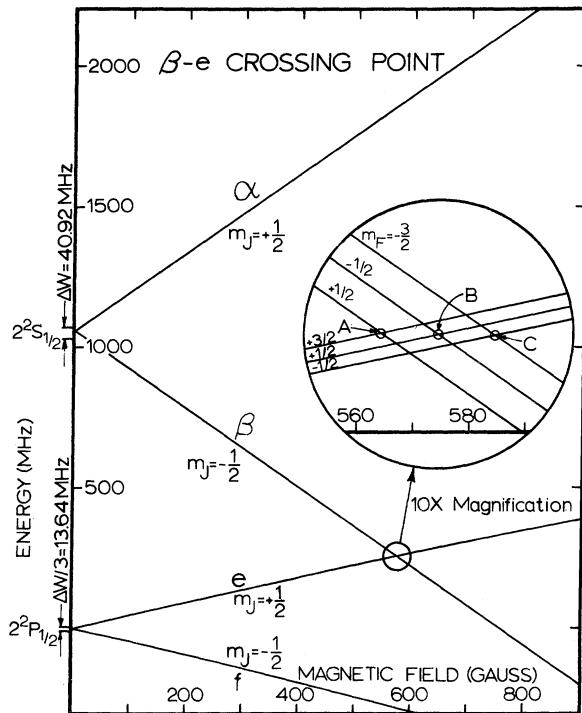


FIG. 2. Zeeman diagram of the $2^2S_{1/2}$ and $2^2P_{1/2}$ levels in D. The inset shows the hfs near the β - e crossing point. In these experiments, the crossings labelled B and C are observed.

netic field. A state selector is used to regenerate any single desired hfs component of the $2S$ state β from the α -state beam. A pair of electrodes located at the center of the main magnetic field provides a well-localized transverse electric field. This field provides the electric dipole coupling necessary to induce transitions between the states β and e . A detector monitors the number of metastable atoms surviving transit through the machine. The β - e crossing point is determined by observing the resonant depletion of the metastable beam. The Lamb shift is calculated from the crossing-point magnetic field measurement and Zeeman energy formulas.

The apparatus used in these experiments is shown schematically in Fig. 3. The oven, electron gun, Helmholtz coil, and detector are described in Ref. 1. The flopper consists of a solenoid which provides a small, static, axial magnetic field at the site of the beam. A small five-turn coil is located inside the solenoid to provide an axial radio-frequency magnetic field. The entire assembly is magnetically shielded from the nearby electron-gun collimating magnet and the Helmholtz coil.

To produce atoms in the state β_C (see Fig. 4) the solenoid is set to produce a small negative⁵ magnetic field. No rf magnetic field is used. This field configuration produces a "sudden" change in the axis of quantization experienced by the α -state beam as it emerges from the electron gun. We calculate that 29.2% of the entering α -

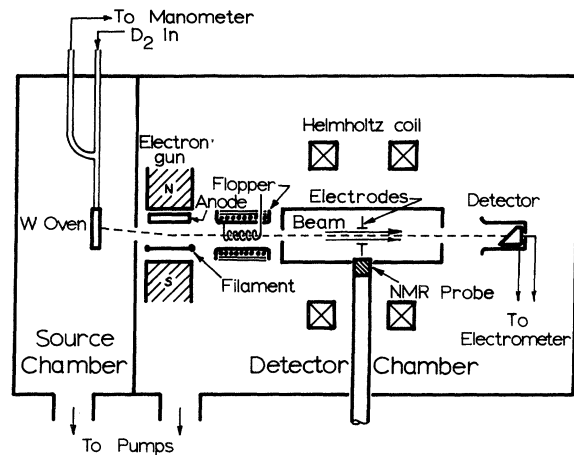


FIG. 3. Schematic diagram of the apparatus. The NMR probe is inserted into the quenching region between the electrodes during field measurements.

state beam should be converted to the state β_C by this nonadiabatic process. The average observed conversion ratio was $(29.7 \pm 2.9)\%$.

To produce atoms in the state β_B , the solenoid is set to produce a magnetic field of +4.9 G. At this field, the levels α_3 and β_B are separated by the minimum frequency of 38,578 MHz. The rf magnetic field is set to this frequency, and its amplitude is adjusted to give the maximum α_3 - β_B conversion.

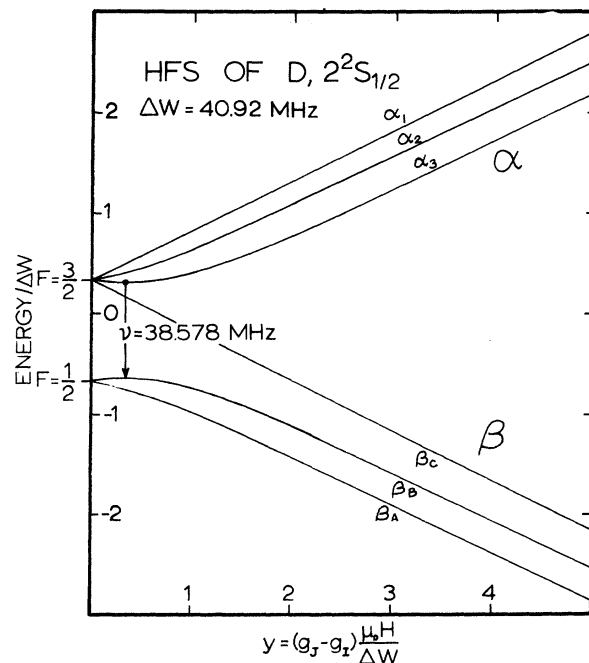


FIG. 4. Hyperfine structure of D, $2^2S_{1/2}$. The arrow indicates the transition that is induced to produce the β_B state. This is done at $y = 1/3$ (or $H \approx 4.9$ G) and $\nu = 38,578$ MHz.

III. THE NATURE OF THE DATA

In seven different runs, a total of 128 measurements of crossing point B were obtained. 117 measurements of crossing point C were obtained in six runs. During each run a complete resonance curve was taken. Figure 5 shows one of these curves where the experimental points are compared with a theoretical resonance curve.

The theoretical curve shown was obtained by using the Bethe-Lamb theory of the $2S$ lifetime, and has been averaged over a v^2 Maxwell velocity distribution in the metastable beam. This curve was fitted only to the peak point by selection of the maximum fractional quenching (F_M) and the crossing-point magnetic field. The gross agreement with the data points is good.

Data for determining the center of this resonance curve were accumulated by measuring the beam quenching at the steepest part of the resonance curve many times. These measurements were made at $\frac{3}{4}F_M$. A measurement of the beam flop at each of the upper and lower such points yielded 1 value of the center. There were generally small differences in the beam flop between these upper and lower "working points." Equalized beam flops were obtained by extrapolating from the observed beam flops along the measured line slope. The value for the center was then taken as the magnetic field midway between these equalized points. A number of small corrections had to be applied to this observed resonance center, and these will be discussed in some detail later in this article.

IV. THE RESONANCE LINE SHAPE

The Bethe-Lamb theory for the lifetime of the $2S$ state under an external perturbation is used to obtain a line shape for the β - e transition resonance. This has already been discussed in some detail in Ref. 1. We present a brief summary of the results here.

The change in beam that is observed when a perturbing electric field E is applied to the beam is given by

$$\Delta B(E, \nu) \approx B_0(\nu) \times \left[1 - \exp \left(-\frac{D}{v\tau_P} \frac{(E/E_0)^2}{1 + \kappa_0^2(\nu-1)^2} K(\nu) \right) \right], \quad (1)$$

where ν is the magnetic field variable $\nu = H/H_x$; H_x is the crossing-point magnetic field; E is the electric field experienced by the atoms; and $E_0 = 22.5$ V/cm is a scale field for $2S$ - $2P$ quenching. D is an effective length for the quenching region ($D = 0.56$ cm for our electrodes), and κ_0 is a dimensionless constant that depends only slightly upon the particular crossing-point ($\kappa_0 \approx 21$). The factor $K(\nu)$ corrects the simple Lorentzian exponential for curvature of the Zeeman fs and hfs lines, for variation of the Stark matrix element, and for the finite spatial extent of the quenching region. $K(\nu)$ is very nearly linear in magnetic field, and can be written for the deuterium crossing points as

$$K(\nu) \approx 1 + 6.7 \times 10^{-2}(\nu - 1). \quad (2)$$

This line-shape theory is tested by comparison with the experimentally observed half-widths and working point slopes. The ratios of the experimentally observed half-widths to the theoretical half-widths ($\delta H_E/\delta H_T$) for the two crossing-points are

$$\text{Crossing point } B: \delta H_E/\delta H_T = 0.995 \pm 0.017,$$

$$\text{Crossing point } C: \delta H_E/\delta H_T = 1.002 \pm 0.010.$$

The ratios of the experimental working point slopes to the theoretical slopes (m_E/m_T) for the two crossing points are

$$\text{Crossing point } B: m_E/m_T = 1.041 \pm 0.046,$$

$$\text{Crossing point } C: m_E/m_T = 0.993 \pm 0.040.$$

Each of these figures is obtained by taking weighted averages from all the runs included in the final data. Each error quoted is one standard deviation. The maximum quenching of these resonance curves ranged from 0.2086 to 0.4647.

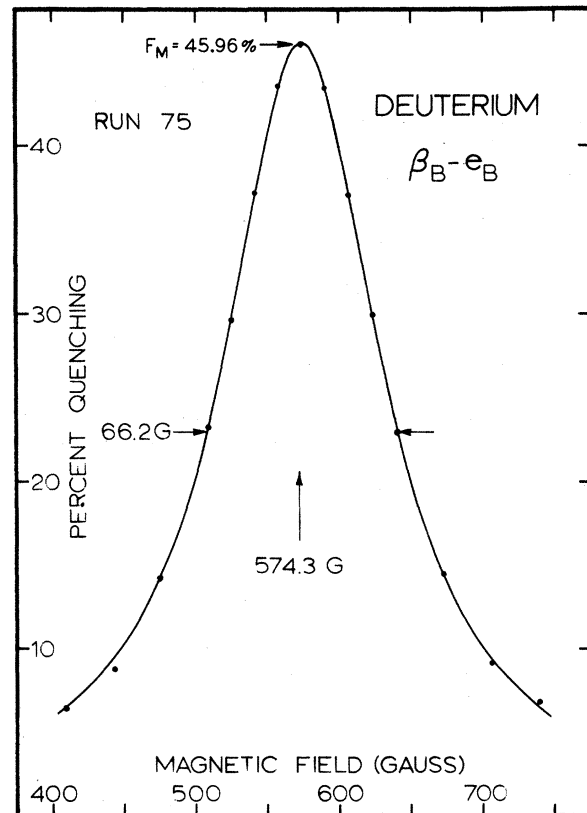


FIG. 5. Resonance curve for crossing point B . The experimental points are plotted along with a line shape derived from the Bethe-Lamb theory of the lifetime of the $2S$ level. The line shape has been averaged over a v^2 beam velocity distribution.

V. CORRECTIONS TO THE DATA

The observed resonance centers are shifted from the true β - e crossing-point magnetic fields by small but significant amounts. We will first discuss some corrections which are common to all of the β - e crossing points and then corrections which only apply to specific crossing points.

A. Stark Matrix Element Variation

The e state is coupled to the $2^2P_{3/2}$ ($m_J = +\frac{1}{2}$) level b by the $\vec{L} \cdot \vec{S}$ interaction. Consequently, $\langle e |$ and hence $\langle e | e \vec{E} \cdot \vec{r} | \beta \rangle$ are magnetic-field dependent. This causes an increase of $\approx 5\%$ in the beam quenching as the magnetic field is varied across the resonance. This asymmetry causes the apparent center to be ≈ 65 ppm above the true center.

B. Level Curvature

As we have just noted the e -state wave function varies with magnetic field. This manifests itself as a curvature of this f_s Zeeman level in a magnetic field. The β f_s state is perfectly linear in magnetic field. The quenching of the metastable atoms at low levels is proportional to $[1 + A(E_\beta - E_e)^2]^{-1}$, and as a result of level curvature this quenching is not symmetric about the β - e crossing point. There is an analogous asymmetry due to the curvature of the hfs levels that results from the $\vec{I} \cdot \vec{J}$ interaction. Level curvature asymmetries shift the apparent resonance center about 10 ppm above the true center.

C. α - f Transitions

The metastable beam consists of approximately two-thirds α -state atoms which undergo transitions to the f state via the same electric dipole interaction that couples states β and e . Near 574 G the α - f transition frequency is approximately 2200 MHz. Since the β - e crossing-point frequency of 0 Hz is far removed from the α - f transition frequency, we approximate the effect of this α background by taking the first term only in an expansion of the α - f quenching. Thus for a given quench level $Q \equiv E/E_0$ we can write the beam flop as

$$\Delta B(r) \approx B_0(r) \left[1 - \exp\left(-\frac{D}{v\tau_P} \frac{Q^2}{1 + \kappa_0^2(r-1)^2}\right) + \frac{2(D/v\tau_P)Q^2}{1 + (4\pi\tau_P v \nu_{\alpha f})^2} \right]. \quad (3)$$

The total β signal is obtained by extrapolating from the sloping "plateau" of a beam quenching curve as shown in Fig. 6. Since this curve shows beam quenching versus the square of the applied voltage, to the order of this perturbation calculation, a linear extrapolation exactly accounts for the α component. A correction is made for the error involved in this extrapolation. This, along with the variation in the α - f background transition rate with magnetic field, causes the

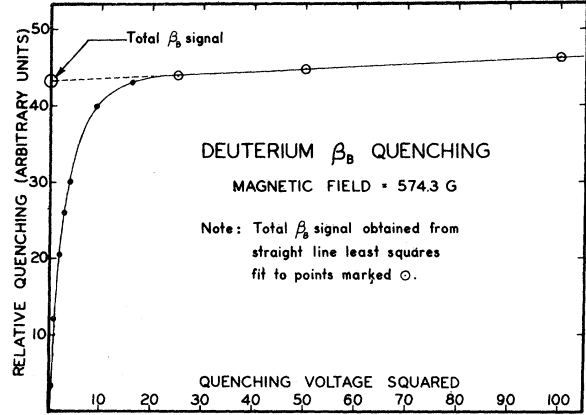


FIG. 6. Metastable deuterium quenching. The sloping plateau is due to the α -state component of the metastable beam.

apparent center of the β - e resonance curve to appear about 10 ppm above the true center.

D. Stark Shift

The applied electric field as well as the much smaller motional electric field couples the β level to the levels b and d , and the e level to the level α via the quadratic Stark interaction. The net effect of these shifts is to cause the center of the resonance curve to appear about 0.3 ppm above the true center.

The Wigner-von Neumann "no-crossing" theorem does not apply in this experiment⁶ since the perturbing electric field is small ($\ll 11.2$ V/cm for this case). The Stark-effect direct coupling of the levels β and e does not shift the center of the resonance curve. A slight symmetrical narrowing of the resonance curve does occur, but was not studied in detail.

E. Velocity Distribution Distortion

The metastable beam diverges slightly and may be tilted with respect to the coil magnetic axis by angles up to $\sim 1^\circ$. Thus small motional electric fields are continually present at the site of the beam. These motional electric fields effectively reduce the speed of the metastable beam by preferentially quenching the faster metastable atoms. The detector signal thus arises from the slower metastable atoms that were in the quenching region for a longer period of time. These atoms are quenched more heavily. The transition resonance then appears about 80 ppm higher in field than it would were these fields absent.

In the analysis of this effect, the quenching is artificially separated into that due to motional fields arising from the gross tilt of the beam and motional fields due to transverse components of the Helmholtz coil field. The quenching due to these motional fields is then calculated by averaging over the beam path length, a Helmholtz field, and a v^2 beam velocity distribution.

Details of this calculation are given in Ref. 3.

F. Finite Extent of the Quenching Region

Some of the electric field does extend over a finite amount of beam path length, and thus some of the beam quenching occurs at magnetic fields lower than the central field. The mean quenching occurs at a slightly lower field than the measured central field. This mean quenching then becomes resonant when the central field of the coil is 26 ppm greater than the true crossing-point field.

G. Hydrogen Impurities

Measurements of crossing point C are sensitive to hydrogen impurity in the deuterium beam. Hydrogen in the beam undergoes nonadiabatic transitions in the flopper into the $\beta(m_F = -1)$ state, and has the hydrogen $\beta_B - e_B$ crossing point resonance at ≈ 605 G.¹ The effective hydrogen component in the beam⁷ is measured in the following manner: With a known deuterium β_C beam, the flopper is set to produce hydrogen metastable atoms in the state $\beta(F=0, m_F=0)$. This is done by setting the flopper solenoid to produce a field of +3 G and by setting the radio frequency to 177.8 MHz. Under these conditions, a hydrogen β_B beam is produced; but no deuterium β states are produced at all, since the hfs separation is much different from that of hydrogen. The Helmholtz coil field is set to the hydrogen $\beta_A - e_A$ crossing point² at 538 G and the hydrogen β_A beam is measured. The effective hydrogen β_B component of the deuterium β_C beam is deduced from this hydrogen β_A signal and the known $\alpha \rightarrow \beta_A$ and $\alpha \rightarrow \beta_B$ conversion ratios in hydrogen.

This measurement was made in each of the $\beta_C - e_C$ runs (the same tank³ of D_2 was used throughout), and in a special run at the end of the series. The weighted average value for N_H/N_D , the ratio of hydrogen β_B metastable atoms to deuterium β_C metastable atoms was

$$N_H/N_D = (1.86 \pm 0.21) \times 10^{-2}. \quad (4)$$

A complete $\beta_C - e_C$ crossing point run was taken for calibration using a mass-spectrometer analyzed mixture of H and D having $N_H/N_D = 10.70 \times 10^{-2}$. The uncorrected center for this run appeared at 2489.973 ± 0.167 kHz proton NMR in water.⁹ For each run, the uncorrected center was scaled down to zero H component in the beam. An uncertainty of 50% of the size of the correction was added to each value. The mean correction added to each center was -169 ± 85 ppm. There is no hydrogen impurity correction to be added to the β_B crossing-point measurements.

H. β Impurities

To produce deuterium atoms in the state β_B , a radio frequency of 38.578 MHz is applied to the beam at a magnetic field of +4.9 G in the flopper. Under these conditions there is a slight overlap with the $\alpha_2 \rightarrow \beta_A$ transition at ~ 47.2 MHz which

produces a small β_A contamination of the β_B beam. This produces a $\beta_A - e_A$ crossing-point resonance at ~ 564 G. This shifts the apparent center of the $\beta_B - e_B$ resonance downward by 14 ppm.

I. Forbidden Transitions

The level β_B is coupled to the level α_3 by the hfs interaction $\vec{I} \cdot \vec{J}$.¹⁰ The level α_3 is coupled to e_C by the Stark interaction $e\vec{E} \cdot \vec{r}$ due to components of the electric field parallel to the magnetic field. There is a similar coupling of levels β_B and e_C through the level $f(m_F = -\frac{1}{2})$. The resulting pseudocrossing of the levels β_B and e_C overlaps the $\beta_B - e_B$ crossing-point resonance curve. The ratio of the amplitude of this "forbidden" transition to the amplitude of the allowed $\beta_B - e_B$ transition is given by second-order degenerate perturbation theory¹¹ as

$$R = \frac{1}{|V_{\beta e}|^2} \sum_i \left| \frac{V_{\beta i} V_{ie}}{E_{\beta} - E_i} \right|^2, \quad i = \alpha, f. \quad (5)$$

We estimate the parallel component of the electric field to be $0.1 \times E_Q$. We calculate $R = 2.3 \times 10^{-6}$. This pseudocrossing appears only about 3 G above the $\beta_B - e_B$ crossing. Thus the fractional shift of the crossing-point magnetic field is ~ 2 parts in 10^8 . There is no effect on crossing point C .¹²

J. β - f Transitions

Small components of the electric field are parallel to the magnetic field. These parallel components induce transitions from state β to state f . Because the levels are well separated and because the parallel field components are small, this decay channel causes the apparent crossing point to be only ~ 1 ppm above the true resonance center.

K. Motional Field Quenching

If the beam is tilted with respect to the coil axis, an asymmetrizing effect arises from the resulting motional electric field. The quenching is proportional to

$$\begin{aligned} |\vec{E}_{\text{tot}}|^2 &= (\vec{E}_Q + \vec{E}_{\text{mot}})^2 \\ &= E_Q^2 + 2\vec{E}_Q \cdot \vec{E}_{\text{mot}} + (E_{\text{mot}})_{\text{av}}^2. \quad (6) \end{aligned}$$

The cross term is linear in magnetic field and can either increase or decrease E^2 depending upon the beam orientation. We experimentally average the effect of this term to zero by reversing the polarity of E_Q at 25 Hz. The effect of motional fields upon the velocity distribution has already been discussed.

VI. THE RESULTS

During each run an average value for the center was obtained. A total correction was determined according to the particular machine parameters of each run and was then added to the raw center for that run. Average values for the individual corrections are listed in Table I. The corrected

TABLE I. Asymmetry corrections added to centers.

Title	Crossing point B (ppm)	Crossing point C (ppm)
Stark matrix-element variation	-63	-66
Level curvature	-10	-10
α - f transitions	-10.4	-8.8
Stark shift	-0.3	-0.3
Velocity distribution distortion	-81 \pm 20	-80 \pm 20
Finite size of the quench region	-26	-26
Hydrogen impurities	0	-169 \pm 85
β impurities	+14	0
Forbidden transitions	\sim 0	0
β - f transitions	-0.7	-0.9
Motional field quenching	0	0
Total	-177 \pm 20	-361 \pm 87

centers are then used with the theory of Brodsky and Parsons¹³ to calculate the Lamb shift. For crossing point B , the weighted, averaged uncorrected center is 2444.648 kHz proton NMR in water to which is added a total correction of -0.433 kHz (-177 \pm 20 ppm). Thus the corrected center and the Lamb shift calculated from the Brodsky-Parsons theory are

$$f_B = 2444.215 \text{ kHz} (\pm 0.097 \text{ kHz} = 40 \text{ ppm}),$$

$$s = 1059.288 \text{ MHz.} \quad (7)$$

Similarly for crossing point C , we observed a weighted, averaged uncorrected center of 2487.973 kHz and a total correction of -0.898 kHz (-361 \pm 87 ppm). This then gives

$$f_C = 2487.075 \text{ kHz} (\pm 0.129 \text{ kHz} = 52 \text{ ppm}),$$

$$s = 1059.165 \text{ MHz.} \quad (8)$$

The errors quoted for the corrected centers are each one standard deviation of the mean and include estimated errors in the correction terms. Weighing each of these values according to σ^{-2} , we obtain the final result for the Lamb shift in the $n = 2$ level in deuterium:

$$s = 1059.24 \pm 0.10 \text{ MHz,} \quad (9)$$

where the quoted error is three times the standard deviation of the mean and is intended to be an es-

timate of the limit of error for this experiment.

This result is to be compared with the original measurement by Triebwasser, Dayhoff, and Lamb.⁴ Their result of 1059.00 ± 0.10 MHz disagrees with the result of this experiment by 0.24 ± 0.14 MHz. The origin of this disagreement is not known. The theoretical value for this Lamb shift has been calculated by Erickson and Yennie¹⁴ and Soto¹⁵ using the recent value of the fine structure constant α obtained by Parker, Taylor, and Langenberg.¹⁶ Their theoretical result for deuterium is

$$s_{th} = 1058.83 \pm 0.08 \text{ MHz.} \quad (10)$$

A correction to this result, due to a possible "proton halo," has been calculated by Barrett, Brodsky, Erickson, and Goldhaber,¹⁷ which raises the value in (10) by 0.25 MHz, giving the result

$$s_{th} = 1059.08 \pm 0.14 \text{ MHz.} \quad (11)$$

Using this result, the discrepancy between theory and this experiment is

$$s_{exp} - s_{th} = +0.16 \pm 0.17 \text{ MHz.} \quad (12)$$

The theoretical difference between the Lamb shifts in the $n = 2$ levels of deuterium and hydrogen^{14,15} is

$$s(D) - s(H) = 1.26 \pm 0.20 \text{ MHz (theory).} \quad (13)$$

The result of this experiment along with Robiscoe's corrected result from the hydrogen level crossing experiments³ gives

$$s(D) - s(H) = 1.38 \pm 0.14 \text{ MHz (experiment),} \quad (14)$$

which agrees with the theoretical result to within the quoted errors.

This experiment has remeasured the Lamb shift in the $n = 2$ level of deuterium and has obtained a result that disagrees slightly with the original Lamb result but agrees within the quoted errors with the most recent theoretical predictions.

VII. ACKNOWLEDGMENTS

I wish to thank W. L. Lichten and R. T. Robiscoe for their valuable support and guidance during the course of this work. I wish to thank R. Reno for many valuable discussions and for help in taking data. Thanks also go to T. Vorburger and T. Wik for their assistance.

*Research supported in part by the National Science Foundation.

† Presented as a dissertation for the degree of Doctor of Philosophy at Yale University.

¹R. T. Robiscoe, Phys. Rev. **138**, A22 (1965).

²R. T. Robiscoe and B. L. Cosens, Phys. Rev.

Letters **17**, 69 (1966).

³R. T. Robiscoe, Phys. Rev. **168**, 4 (1968).

⁴S. Triebwasser, E. S. Dayhoff, and W. E. Lamb, Jr., Phys. Rev. **89**, 98 (1953).

⁵Positive is defined as the direction of the beam velocity. The Helmholtz coil provides a magnetic field in the positive direction.

⁶W. E. Lamb, Jr., Phys. Rev. **85**, 259 (1952). See pp. 272-273.

⁷The hydrogen component in the beam is presumably different from the hydrogen component in the tank because of such effects as differences in recoil angles in the electron gun and differences in velocity.

⁸The deuterium was purchased from Bio-Rad Laboratories, Richmond, California. They claimed a purity of 99.65-99.8 atom % D.

⁹All magnetic fields are expressed in terms of the resonance frequency of the proton NMR probe.

¹⁰See Ref. 6, Eq. (174).

¹¹See L. D. Landau and E. M. Lifshitz, *Quantum Mechanics* (Addison-Wesley Publishing Company, Inc., Reading, Mass., 1958), p. 139, Eq. (3).

¹²See M. Leventhal, Phys. Letters **20**, 6. 1 April, 1966, pp. 625-627, for an observation of a similar forbidden transition.

¹³S. J. Brodsky and R. G. Parsons, Phys. Rev. **163**, 134-146 (1967). They claim an inherent accuracy of 1 ppm for conversion of crossing point NMR frequency to Lamb shift.

¹⁴G. W. Erickson and D. R. Yennie, Part I, Ann. Phys. (N. Y.) **35**, 271 (1965); Part II, Ann. Phys. (N. Y.) **35**, 447 (1965).

¹⁵M. F. Soto, Jr., Phys. Rev. Letters **17**, 1153 (1966).

¹⁶W. H. Parker, B. N. Taylor, and D. N. Langenberg, Phys. Rev. Letters **18**, 287 (1967).

¹⁷R. C. Barrett, S. J. Brodsky, G. W. Erickson, and M. H. Goldhaber, to be published.

2P Π States of Muonic Molecules*

Benjamin P. Carter

*Lawrence Radiation Laboratory, University of California,
Livermore, California*

(Received 29 January 1968)

The possible existence of μ -molecular states corresponding to the 2P Π muon orbital is investigated. Such states are found to be bound in the lowest adiabatic approximation, with levels near the $n=2$ atomic levels.

I. INTRODUCTION

After slowing down in liquid hydrogen, a negative muon (μ) undergoes a sequence of chemical reactions which result in the formation of a muonic protium ($p\mu$), deuterium ($d\mu$), or tritium ($t\mu$) atom of low principal quantum number n . The reaction rates have been computed by Wightman¹ and (for pions) by Leon and Bethe.² For muons, the estimates of Ref. 2 indicate that Auger transitions dominate in the de-excitation down to $n=3$, but that Auger rates are small compared to radiative rates for transitions with a final n of 1 or 2. After the atom reaches the ground ($n=1$) state, subsequent interactions with other nuclei can involve only those molecular-ion states ($p\mu p$, $p\mu d$, etc.) which correspond to a 1S Σ orbital³ of the muon. These (and only these) states have been extensively studied by adiabatic approximations⁴ and by the variational method.⁵

In this paper we investigate the possibility that three-body states corresponding to the 2P Π muon orbital⁶ may play a role in the interaction between an excited muonic atom and a hydrogen nucleus. We show (Sec. IV) that in the lowest-order adiabatic approximation, there do exist 2P Π levels which lie close to the $n=2$ atomic levels. This means that we may expect resonances (near the 2P Π levels) in the scattering of an atom off a nucleus. It is also probable that there exist bound even-parity molecular-ion states of angular momentum 1. Bhatia and Temkin have shown that these three-body states correspond to Π orbitals,⁷ of which the 2P Π has the lowest energy. To obtain

even parity in an adiabatic approximation we must consider the two nuclei to be in a relative P state. This introduces a centrifugal term which must be added to the adiabatic Born-Oppenheimer potential. We calculate energy levels both with and without the centrifugal term; these cases approximate even- and odd-parity three-body states, respectively.

II. THREE-BODY HAMILTONIAN

Let m_1 and m_2 be the masses of two nuclei (each an isotope of hydrogen) and m_3 be the muon mass. We use reduced muonic units, i. e., atomic units, with respect to the reduced mass

$$m = m_3(m_1 + m_2) / (m_1 + m_2 + m_3). \quad (1)$$

In these units the three-body Hamiltonian (excluding the kinetic energy of the center of mass) is

$$H = -\frac{1}{2}\nabla_r^2 - \nabla_R^2 / 2M + 1/R - 1/r_1 - 1/r_2. \quad (2)$$

The symbols in (2) have the following meanings. r_1 and r_2 are the distances of the muon from nuclei 1 and 2. The first gradient is with respect to the displacement \vec{r} of the muon from the center of mass of the nuclei. The second gradient is with respect to the displacement \vec{R} of nucleus 2 from nucleus 1. The dimensionless parameter M is the reduced mass of the two nuclei in units of m :

$$M = m_1 m_2 / m(m_1 + m_2). \quad (3)$$

Table I shows the values of M used in the present work, as well as the factor m/m_e which is needed